

In the previous chapter we learned that the restricted Delaunay triangulation is a good approximation of a densely sampled surface  $\Sigma$  from both topological and geometric view point. Unfortunately, we cannot compute this triangulation because the restricted Voronoi diagram  $\text{Vor } P|_{\Sigma}$  cannot be computed without knowing  $\Sigma$ . As a remedy we approximate the restricted Voronoi diagram and compute a set of triangles that is a superset of all restricted Delaunay triangles. This set is pruned to extract a manifold surface which is output as an approximation to the sampled surface  $\Sigma$ .

### 4.1 Algorithm

First, we observe that each restricted Voronoi cell  $V_p|_{\Sigma} = V_p \cap \Sigma$  is almost flat if the sample is sufficiently dense. This follows from the Normal Variation Lemma 3.3 as the points in  $V_p|_{\Sigma}$  cannot be far apart if  $\varepsilon$  is small. In particular,  $V_p|_{\Sigma}$  lies within a thin neighborhood of the tangent plane  $\tau_p$  at  $p$ . So, we need two approximations: (i) an approximation to  $\tau_p$  or equivalently to  $\mathbf{n}_p$  and (ii) an approximation to  $V_p|_{\Sigma}$  based on the approximation to  $\mathbf{n}_p$ . The following definitions of *poles* and *cocones* are used for these two approximations.

#### 4.1.1 Poles and Cocones

**Definition 4.1 (Poles).** *The farthest Voronoi vertex, denoted  $p^+$ , in  $V_p$  is called the positive pole of  $p$ . The negative pole of  $p$  is the farthest point  $p^- \in V_p$  from  $p$  so that the two vectors from  $p$  to  $p^+$  and  $p^-$  make an angle more than  $\frac{\pi}{2}$ . We call  $\mathbf{v}_p = p^+ - p$ , the pole vector for  $p$ . If  $V_p$  is unbounded,  $p^+$  is taken at infinity and the direction of  $\mathbf{v}_p$  is taken as the average of all directions given by the unbounded Voronoi edges.*

The following lemma is a direct consequence of the Normal Lemma 3.2. It says that the pole vectors approximate the true normals at the sample points.

**Lemma 4.1 (Pole).** *For  $\varepsilon < 1$ , the angle between the normal  $\mathbf{n}_p$  at  $p$  and the pole vector  $\mathbf{v}_p$  satisfies the inequality*

$$\angle_a(\mathbf{n}_p, \mathbf{v}_p) \leq 2 \arcsin \frac{\varepsilon}{1 - \varepsilon}.$$

*Proof.* First, consider the case where  $V_p$  is bounded. Since the Voronoi cell  $V_p$  contains the centers of the medial balls at  $p$ , we have  $\|p^+ - p\| \geq f(p)$ . Thus, plugging  $\mu = 1$  in the Normal Lemma 3.2 we obtain the result immediately.

Next, consider the case where  $V_p$  is unbounded. In this case  $\mathbf{v}_p$  is computed as the average of the directions of the infinite Voronoi edges. The angle  $\angle_a(\mathbf{v}_p, \mathbf{n}_p)$  in this case cannot be more than the worst angle made by an infinite Voronoi edge with  $\mathbf{n}_p$ . An infinite Voronoi edge  $e$  makes the same angle with  $\mathbf{n}_p$  as the vector  $\overrightarrow{pp_\infty}$  does, where the infinite endpoint of  $e$  is taken at  $p_\infty$ . Again we have  $\|p - p_\infty\| \geq f(p)$  and the Normal Lemma 3.2 can be applied with  $\mu = 1$  to give the result. ■

The Pole Lemma 4.1 says that the pole vector approximates the normal  $\mathbf{n}_p$ . Thus, the plane  $\tilde{\tau}_p$  passing through  $p$  with the pole vector as normal approximates the tangent plane  $\tau_p$ . The following definition of *cocone* accommodates a thin neighborhood around  $\tilde{\tau}_p$  to account for the small uncertainty in the estimation of  $\mathbf{n}_p$ .

**Definition 4.2 (Cocone).** *The set  $C_p = \{y \in V_p : \angle_a(\overrightarrow{py}, \mathbf{v}_p) \geq \frac{3\pi}{8}\}$  is called the cocone of  $p$ . In words,  $C_p$  is the complement of a double cone that is clipped within  $V_p$ . This double cone has  $p$  as the apex, the pole vector  $\mathbf{v}_p$  as the axis, and an opening angle of  $\frac{3\pi}{8}$  with the axis. See Figure 4.1 for an example of a cocone.*

As an approximation to  $V_p|_\Sigma$ , cocones meet all Voronoi edges that are intersected by  $\Sigma$ . So, if we compute all triangles dual to the Voronoi edges intersected by cocones, we obtain all restricted Delaunay triangles and possibly a few others. We call this set of triangles *cocone triangles*. We will see later that all cocone triangles lie very close to  $\Sigma$ . A cleaning step is necessary to weed out some triangles from the set of cocone triangles so that a 2-manifold is computed as output. This is accomplished by a *manifold extraction* step.

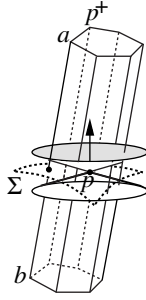


Figure 4.1. The positive pole  $p^+$  helps estimating the normal. The double cone forming the cocone has the apex at  $p$  and axis  $pp^+$ . The Voronoi edge  $ab$  intersects the cocone. Its dual Delaunay triangle is a cocone triangle.

### COCONE( $P$ )

```

1  compute Vor  $P$ ;
2   $T = \emptyset$ ;
3  for each Voronoi edge  $e \in \text{Vor } P$  do
4    if COCONETRIANGLES( $e$ )
5       $T := T \cup \text{dual } e$ ;
6  endfor
7   $E := \text{EXTRACTMANIFOLD}(T)$ ;
8  output  $E$ .
```

Let us now look into the details of the two steps COCONETRIANGLES and EXTRACTMANIFOLD.

To check if a Voronoi edge  $e = (a, b)$  intersects  $C_p$  we consider the three vectors  $\mathbf{v}_p$ ,  $\mathbf{a} = \overrightarrow{pa}$ ,  $\mathbf{b} = \overrightarrow{pb}$ , and three conditions I, II, and III:

$$\begin{aligned}
 \text{I. } & \frac{|\mathbf{v}_p^T \mathbf{a}|}{\|\mathbf{v}_p\| \|\mathbf{a}\|} \leq \cos \frac{3\pi}{8} \quad \text{or} \quad \frac{|\mathbf{v}_p^T \mathbf{b}|}{\|\mathbf{v}_p\| \|\mathbf{b}\|} \leq \cos \frac{3\pi}{8}, \\
 \text{II. } & \frac{\mathbf{v}_p^T \mathbf{a}}{\|\mathbf{v}_p\| \|\mathbf{a}\|} < 0 \quad \text{and} \quad \frac{-\mathbf{v}_p^T \mathbf{b}}{\|\mathbf{v}_p\| \|\mathbf{b}\|} < 0, \\
 \text{III. } & \frac{\mathbf{v}_p^T \mathbf{a}}{\|\mathbf{v}_p\| \|\mathbf{a}\|} > 0 \quad \text{and} \quad \frac{-\mathbf{v}_p^T \mathbf{b}}{\|\mathbf{v}_p\| \|\mathbf{b}\|} > 0.
 \end{aligned}$$

Condition I checks if any of the vertices  $a$  and  $b$  of the Voronoi edge  $e$  lies inside  $C_p$ . Conditions II and III check if both  $a$  and  $b$  lie outside  $C_p$ , but the edge  $e$  crosses it. The triangle  $t = \text{dual } e$  is marked as a cocone triangle only if  $e$  intersects cocones of *all* three vertices of  $t$ .

COCONETRIANGLES( $e$ )

```

1   $t := \text{dual } e$ ;
2   $\text{flag} := \text{TRUE}$ ;
3  for each vertex  $p$  of  $t$  do
4    if none of Conditions I, II, and III holds
5       $\text{flag} := \text{FALSE}$ ;
6  endfor
7  return  $\text{flag}$ .
```

The set  $T$  of cocone triangles enjoys some interesting geometric properties which we exploit in the manifold extraction step as well as in the proofs of geometric and topological guarantees of COCONE. Of course, the sample has to be sufficiently dense for these properties to hold. In the rest of the chapter we assume that  $\varepsilon \leq 0.05$  which satisfies Condition A stated in Chapter 3, enabling us to apply the results therein.

#### 4.1.2 Cocone Triangles

First, we show that each triangle in  $T$  has a small empty ball circumscribing it, that is, the radius of this ball is small compared to the local feature sizes at their vertices. Notice that the diametric ball of a triangle may not be empty. Hence, the smallest *empty* ball circumscribing a triangle may not be its diametric ball. Nevertheless, a small empty circumscribing ball also means that the circumradius of the triangle is small. This fact together with the Triangle Normal Lemma 3.5 implies that all cocone triangles lie almost flat to the surface.

**Lemma 4.2 (Small Triangle).** *Let  $t$  be any cocone triangle and  $r$  denote the radius of the smallest empty ball circumscribing  $t$ . For each vertex  $p$  of  $t$  and  $\varepsilon \leq 0.05$ , one has*

- (i)  $r \leq \frac{1.18\varepsilon}{1-\varepsilon} f(p)$  and
- (ii) *circumradius of  $t$  is at most  $\frac{1.18\varepsilon}{1-\varepsilon} f(p)$ .*

*Proof.* Let  $z$  be any point in  $V_p$  so that

$$\angle_a(n_p, \vec{pz}) \geq \frac{3\pi}{8} - 2 \arcsin \frac{\varepsilon}{1-\varepsilon}. \quad (4.1)$$

First, we claim that for any such point  $z$ , we have  $\|z - p\| \leq \frac{1.18\varepsilon}{1-\varepsilon} f(p)$  if  $\varepsilon \leq 0.05$ .

If  $\angle_a(\mathbf{n}_p, \vec{pz}) > \theta = \arcsin \frac{\varepsilon}{\mu(1-\varepsilon)} + \arcsin \frac{\varepsilon}{1-\varepsilon}$ , then  $\|z - p\| \leq \mu f(p)$  according to the Normal Lemma 3.2. With  $\mu = \frac{1.18\varepsilon}{1-\varepsilon}$  and  $\varepsilon \leq 0.05$  we have

$$\theta = \arcsin \frac{1}{1.18} + \arcsin \frac{\varepsilon}{1-\varepsilon} < \frac{3\pi}{8} - 2 \arcsin \frac{\varepsilon}{1-\varepsilon}. \quad (4.2)$$

Thus, from Inequalities 4.1 and 4.2 we have

$$\angle_a(\mathbf{n}_p, \vec{pz}) \geq \frac{3\pi}{8} - 2 \arcsin \frac{\varepsilon}{1-\varepsilon} > \theta. \quad (4.3)$$

Therefore, any point  $z \in V_p$  satisfying Inequality 4.1 also satisfies

$$\|z - p\| \leq \frac{1.18\varepsilon}{1-\varepsilon} f(p).$$

Now let  $t$  be any cocone triangle with  $p$  being any of its vertices and  $e$  = dual  $t$  being its dual Voronoi edge. For  $t$  to be a cocone triangle, it is necessary that there is a point  $y \in e$  so that  $\angle_a(\mathbf{v}_p, \vec{py}) \geq \frac{3\pi}{8}$ . Taking into account the angle  $\angle_a(\mathbf{v}_p, \mathbf{n}_p)$ , this necessary condition implies

$$\angle_a(\mathbf{n}_p, \vec{py}) \geq \frac{3\pi}{8} - 2 \arcsin \frac{\varepsilon}{1-\varepsilon}$$

which satisfies Inequality 4.1. Hence, we have

$$\|y - p\| \leq \frac{1.18\varepsilon}{1-\varepsilon} f(p) \text{ for } \varepsilon \leq 0.05.$$

The ball  $B_{y, \|y-p\|}$  is empty and circumscribes  $t$  proving (i). The claim in (ii) follows immediately from (i) as the circumradius of  $t$  cannot be larger than the radius of any ball circumscribing it. ■

The next lemma proves that all cocone triangles lie almost parallel to the surface. The angle bounds are expressed in terms of  $\alpha(\varepsilon)$  and  $\beta(\varepsilon)$  that are defined in Chapter 3.

**Lemma 4.3 (Cocone Triangle Normal).** *Let  $t$  be any cocone triangle and  $\mathbf{n}_t$  be its normal. For any vertex  $p$  of  $t$  one has  $\angle_a(\mathbf{n}_p, \mathbf{n}_t) \leq \alpha(\frac{2.36\varepsilon}{1-\varepsilon}) + \beta(1.18\varepsilon)$  when  $\varepsilon \leq 0.05$ .*

*Proof.* Let  $q$  be a vertex of  $t$  with a maximal angle of  $t$ . The circumradius of  $t$  is at most  $\frac{1.18\varepsilon}{1-\varepsilon} f(q)$  by the Small Triangle Lemma 4.2. Then, by the Triangle

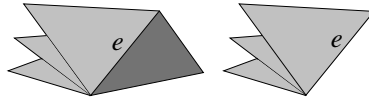


Figure 4.2. The edge  $e$  is not sharp in the left picture; it is sharp in the right picture.

Normal Lemma 3.5,

$$\begin{aligned} \angle_a(\mathbf{n}_q, \mathbf{n}_t) &\leq \arcsin \frac{1.18\varepsilon}{1-\varepsilon} + \arcsin \left( \frac{2}{\sqrt{3}} \sin \left( 2 \arcsin \frac{1.18\varepsilon}{1-\varepsilon} \right) \right) \\ &\leq \arcsin \frac{1.18\varepsilon}{1-1.18\varepsilon} + \arcsin \left( \frac{2}{\sqrt{3}} \sin \left( 2 \arcsin \frac{1.18\varepsilon}{1-1.18\varepsilon} \right) \right) \\ &= \beta(1.18\varepsilon) \text{ for } \varepsilon \leq 0.05. \end{aligned}$$

The distance between  $p$  and  $q$  is no more than the diameter of the circle circumscribing  $t$ , that is,  $\|p - q\| \leq \frac{2.36\varepsilon}{1-\varepsilon} f(p)$  (Small Triangle Lemma 4.2). By the Normal Variation Lemma 3.3,  $\angle(\mathbf{n}_p, \mathbf{n}_q) \leq \alpha(\frac{2.36\varepsilon}{1-\varepsilon})$ . The desired bound for  $\angle_a(\mathbf{n}_p, \mathbf{n}_t)$  follows since it is no more than the sum  $\angle(\mathbf{n}_p, \mathbf{n}_q) + \angle_a(\mathbf{n}_q, \mathbf{n}_t)$ . ■

### 4.1.3 Pruning

Prior to the extraction of a 2-manifold from the set of cocone triangles, some of them are pruned. An edge  $e$  is *sharp* if any two consecutive cocone triangles around it form an angle more than  $\frac{3\pi}{2}$  (see Figure 4.2). Edges with a single triangle incident to them are also sharp by default. We will show later that the cocone triangles include all restricted Delaunay triangles when a sample is sufficiently dense. The set of restricted Delaunay triangles cannot be incident to sharp edges. This implies that we can prune triangles incident to sharp edges and still retain the set of restricted Delaunay triangles. In fact, we can carry out this pruning in a cascaded manner. By deleting one triangle incident to a sharp edge, we may create other sharp edges. Since no restricted Delaunay triangle is pruned, none of their edges become sharp. Therefore, it is safe to delete the new sharp edges with all of their incident triangles.

This pruning step weeds out all triangles incident to sharp edges, but the remaining triangles still may not form a surface. They may form layers of thin pockets creating a nonmanifold. A manifold surface is extracted from this possibly layered set by *walking* outside the space covered by them (see Figure 4.3). The manifold extraction step depends on the fact that cocone triangles contain all restricted Delaunay triangles none of whose edges is sharp. We prove this fact below.

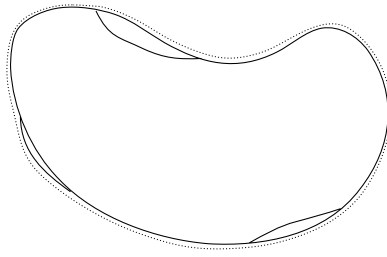


Figure 4.3. Thin pockets left after pruning, a manifold is obtained by walking on the outside indicated by the dotted curve.

**Theorem 4.1 (Restricted Delaunay).** *For  $\varepsilon \leq 0.05$ , the following conditions hold:*

- (i) *cocone triangles contain all restricted Delaunay triangles and*
- (ii) *no restricted Delaunay triangle has a sharp edge.*

*Proof.* Consider (i). Let  $y$  be any point in any restricted Voronoi cell  $V_p|_\Sigma$ . We claim that  $\angle_a(\mathbf{n}_p, \vec{py})$  is larger than  $\frac{\pi}{2} - \arcsin \frac{\varepsilon}{2(1-\varepsilon)}$ . We have  $\|y - p\| \leq \varepsilon f(y)$  since  $y \in V_p|_\Sigma$  and  $P$  is an  $\varepsilon$ -sample of  $\Sigma$ . By the Feature Translation Lemma 1.3,  $\|y - p\| \leq \frac{\varepsilon}{1-\varepsilon} f(p)$ . We can therefore apply the proof of the Edge Normal Lemma 3.4 to establish that

$$\angle_a(\mathbf{n}_p, \vec{py}) \geq \frac{\pi}{2} - \arcsin \frac{\varepsilon}{2(1-\varepsilon)}.$$

Let  $t$  be any restricted Delaunay triangle and  $e = \text{dual } t$  be the dual Voronoi edge. Consider the point  $y = e \cap \Sigma$ . We have  $y \in V_p|_\Sigma$  for each of the three points  $p \in P$  determining  $e$ . For each such  $p$ , the angle  $\angle_a(\mathbf{n}_p, \vec{py})$  is larger than  $\pi/2 - \arcsin \frac{\varepsilon}{2(1-\varepsilon)}$ . Therefore,

$$\begin{aligned} \angle_a(\vec{py}, \mathbf{v}_p) &\geq \angle_a(\vec{py}, \mathbf{n}_p) - \angle_a(\mathbf{n}_p, \mathbf{v}_p) \\ &\geq \frac{\pi}{2} - \arcsin \frac{\varepsilon}{2(1-\varepsilon)} - \angle_a(\mathbf{n}_p, \mathbf{v}_p). \end{aligned} \quad (4.4)$$

By the Pole Lemma 4.1 we have

$$\begin{aligned} \angle_a(\mathbf{n}_p, \mathbf{v}_p) + \arcsin \frac{\varepsilon}{2(1-\varepsilon)} &\leq 2 \arcsin \frac{\varepsilon}{1-\varepsilon} + \arcsin \frac{\varepsilon}{2(1-\varepsilon)} \\ &< \frac{\pi}{8} \text{ for } \varepsilon \leq 0.05. \end{aligned}$$

So, by Inequality 4.4,  $\angle_a(\vec{py}, \mathbf{v}_p) > \frac{3\pi}{8}$ . Therefore, the point  $y$  is in the cocone  $C_p$  by definition. Hence,  $t$  is a cocone triangle.

Consider (ii). Let  $t_1$  and  $t_2$  be adjacent triangles in the restricted Delaunay triangulation with  $e$  as their shared edge and let  $p \in e$  be any of their shared

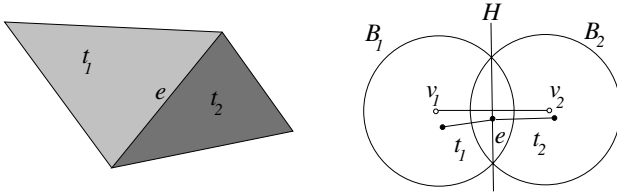


Figure 4.4. Illustration for the Restricted Delaunay Theorem 4.1.

vertices. Since  $t_1$  and  $t_2$  belong to the restricted Delaunay triangulation, they have circumscribing empty balls  $B_1$  and  $B_2$ , respectively, centered at points, say  $v_1$  and  $v_2$  of  $\Sigma$ .

The boundaries of  $B_1$  and  $B_2$  intersect in a circle  $C$  contained in a plane  $H$ , with  $e \subset H$ . The plane  $H$  separates  $t_1$  and  $t_2$ , since the third vertex of each triangle lies on the boundary of its circumscribing ball, and  $B_1 \subseteq B_2$  on one side of  $H$ , while  $B_2 \subseteq B_1$  on the other (see Figure 4.4). The line through  $v_1, v_2$  is perpendicular to  $H$ . Both  $v_1$  and  $v_2$  belong to the Voronoi facet dual to  $e$ . This means  $v_1$  and  $v_2$  belong to a restricted Voronoi cell and the distance  $\|v_1 - v_2\| \leq \frac{2\varepsilon}{(1-\varepsilon)} f(v_1)$  by the Short Distance Lemma 3.6. So, the segment  $v_1 v_2$  forms an angle of at least  $\pi/2 - \arcsin \frac{\varepsilon}{1-\varepsilon}$  with  $\mathbf{n}_{v_1}$  (Edge Normal Lemma 3.4). This normal differs, in turn, from  $\mathbf{n}_p$  by an angle of at most  $\frac{\varepsilon}{1-3\varepsilon}$  (Normal Variation Lemma 3.3). So, the angle between  $H$  and  $\mathbf{n}_p$  is at most  $\frac{\varepsilon}{1-3\varepsilon} + \arcsin \frac{\varepsilon}{1-\varepsilon}$ . For small  $\varepsilon$ , they are nearly parallel. In particular, if  $\varepsilon \leq 0.05$ ,  $H$  makes at most  $7^\circ$  with  $\mathbf{n}_p$ . Similarly, plugging  $\varepsilon \leq 0.05$  in the angle upper bound of the Cocone Triangle Normal Lemma 4.3, one gets that the normals of both  $t_1$  and  $t_2$  differ from the surface normal at  $p$  by at most  $24^\circ$ .

Thus, we have  $t_1$  on one side of  $H$ ,  $t_2$  on the other and the smaller angle between  $H$  and either triangle is at least  $59^\circ$ . Hence, the smaller angle between  $t_1$  and  $t_2$  is at least  $118^\circ$  and  $e$  is not sharp. ■

### 4.1.4 Manifold Extraction

A simplicial complex with an underlying space of a 2-manifold is extracted out of the pruned set of cocone triangles. Let  $\Sigma' \subseteq \Sigma$  be any connected component of the sampled surface. Since cocone triangles are small (Small Triangle Lemma 4.2), they cannot join points from different components of  $\Sigma$ . Let  $T'$  be the pruned set of cocone triangles with vertices in  $\Sigma'$ . Consider the medial axis of  $\Sigma'$ . The triangles of  $T'$  lie much closer to  $\Sigma'$  than to its medial axis. Furthermore,  $T'$  includes the restricted Delaunay triangulation  $\text{Del } P|_{\Sigma'}$  (Restricted Delaunay Theorem 4.1). Therefore, if  $|T'|$  denotes the underlying space of  $T'$ ,



the space  $\mathbb{R}^3 \setminus |T'|$  has precisely two disjoint open sets  $O_{\text{in}}$  and  $O_{\text{out}}$  containing the inner and outer medial axis of  $\Sigma'$  respectively. The manifold extraction step computes the boundary of the closure of  $O_{\text{out}}$ , which we simply refer to as the boundary of  $O_{\text{out}}$ .

Let  $E'$  be the boundary of  $O_{\text{out}}$ . We claim that  $E'$  is a 2-manifold. Let  $p$  be any vertex of  $E'$ . Orient the normal  $\mathbf{n}_p$  so that it points toward  $O_{\text{out}}$ . Consider a sufficiently small ball  $B$  centering  $p$ . Call the point where the ray of  $\mathbf{n}_p$  intersects the boundary of  $B$  the *north pole*. Obviously, the north pole is in  $O_{\text{out}}$ . Let  $T_p$  denote the set of triangles in  $T'$  which are visible from the north pole within  $B$ . The triangles of  $T_p$  are in the boundary of  $O_{\text{out}}$ . Since there is no sharp edge in  $T'$ , the set of triangles  $T_p$  makes a topological disk. We argue that  $T_p$  is the only set of triangles in the boundary of  $O_{\text{out}}$  which are incident to  $p$ .

Let  $q \neq p$  be a vertex of a triangle  $t \in T_p$ . The triangle  $t$  is in  $T_q$ . If not, the line of the normal  $\mathbf{n}_p$ , when moved parallelly through the edge  $pq$  toward  $q$ , must hit an edge in  $T'$  that is sharp. The assumption to this claim is that the normals  $\mathbf{n}_p$  and  $\mathbf{n}_q$  are almost parallel and hence the visibility directions at  $p$  and  $q$  are almost parallel. Since  $T'$  does not have any sharp edge,  $t$  is in  $T_q$ . This means that all topological disks at the vertices of  $E'$  are compatible and they form a 2-manifold. This 2-manifold separates  $O_{\text{out}}$  from  $T'$  implying that  $E'$  cannot have any other triangles from  $T'$  other than the ones in the topological disks described above.

We compute  $E'$  from  $T'$  as a collection of triangles by a depth first walk in the Delaunay triangulation  $\text{Del } P$ . Recall that  $T'$  is disjoint from any other triangles on a component of  $\Sigma$  different from  $\Sigma'$ . The walk starts with a seed triangle in  $T'$ . The routine SEED computes this seed triangle for each component  $T'$  of the pruned set by another depth first walk in the Delaunay triangulation. At any generic step, SEED comes to a triangle  $t$  via a tetrahedron  $\sigma$  and performs the following steps. First, it checks if  $t$  is a cocone triangle. If so, it checks if it belongs to a component  $T'$  for which a seed has not yet been picked. If so, the pair  $(\sigma, t)$ , also called the *seed pair*, is put into the seed set. Then, it marks all triangles of  $T'$  so that any subsequent check can identify that a seed for  $T'$  has been picked. The walk continues through the triangles and their adjacent tetrahedra in a depth first manner till a seed pair for each component such as  $T'$  of  $T$  is found. In a seed pair  $(\sigma, t)$  for a component  $T'$ , the tetrahedron  $\sigma$  and the triangle  $t$  should be in  $O_{\text{out}}$  and on its boundary  $E'$  respectively. To ensure it SEED starts the walk from any convex hull triangle in  $\text{Del } P$  and continues till it hits a cocone triangle. The initiation of the walk from a convex hull triangle ensures that the first triangle encountered in a component is on the outside of that component or equivalently on the boundary of  $O_{\text{out}}$  defined for that component. Assuming the function SEED, a high-level description of EXTRACTMANIFOLD is given.

EXTRACTMANIFOLD( $T$ )

```

1   $T := \text{pruned } T$ ;
2   $SD := \text{SEED}(T)$ ;
3  for each tuple  $(\sigma, t) \in SD$  do
4     $E' := \text{SURFTRIANGLES}(\sigma, t)$ ;
5     $E := E \cup E'$ ;
6  endfor
7  return the simplicial complex of  $E$ .
```

The main task in EXTRACTMANIFOLD is done by SURFTRIANGLES which takes a seed pair  $(\sigma, t)$  as input. First, we initialize the surface  $E'$  with the seed triangle  $t$  which is definitely in  $E'$  (line 1). Next, we initialize a stack *Pending* with the triple  $(\sigma, t, e)$  where  $e$  is an edge of  $t$  (lines 3 and 4). As long as the stack *Pending* is not empty, we pop its top element  $(\sigma, t, e)$ . If the edge  $e$  is not already processed we call the function SURFACENEIGHBOR to compute a tetrahedron–triangle pair  $(\sigma', t')$  (line 9). The tetrahedron  $\sigma'$  is adjacent to  $t'$  and intersects  $O_{\text{out}}$  where  $t'$  is in  $E'$  and is adjacent to  $t$  via  $e$ . The triangle  $t'$  is inserted in  $E'$ . Then two new triples  $(\sigma', t', e')$  are pushed on the stack *pending* for each edge  $e' \neq e$  of  $t'$  (lines 11–13). Finally, we return  $E'$  (line 16).

SURFTRIANGLES( $\sigma, t$ )

```

1   $E' := \{t\}$ ;
2   $Pending := \emptyset$ ;
3  pick any edge  $e$  of  $t$ ;
4  push  $(\sigma, t, e)$  on  $Pending$ ;
5  while  $Pending \neq \emptyset$  do
6    pop  $(\sigma, t, e)$  from  $Pending$ ;
7    if  $e$  is not marked processed
8      mark  $e$  processed;
9     $(\sigma', t') := \text{SURFACENEIGHBOR}(\sigma, t, e)$ ;
10    $E' := E' \cup \{t'\}$ ;
11   for each edge  $e' \neq e$  of  $t'$  do
12     push  $(\sigma', t', e')$  on  $Pending$ ;
13   endfor
14   endif
15 endwhile
16 return  $E'$ .
```

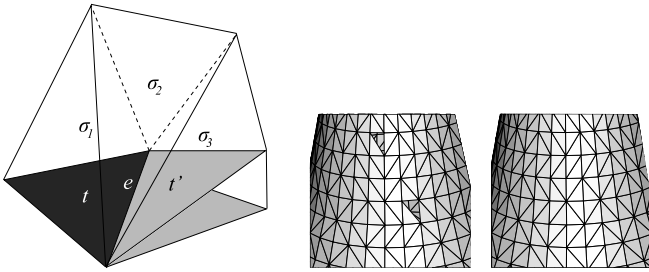


Figure 4.5. A stable computation of SURFACENEIGHBOR (left), a zoom on a reconstruction after an unstable computation with numerical errors (middle), and a stable computation without any numerical error (right).

The question is how to implement the function SURFACENEIGHBOR. It has to output a tuple  $(\sigma', t')$  where  $t'$  is the neighbor of  $t$  on the surface given by  $E'$  and  $\sigma'$  is an adjacent tetrahedron intersecting  $O_{\text{out}}$ . One can compute the surface neighbor  $t'$  of  $t$  using some numerical computations involving some dot product computations of vectors. However, these computations often run into trouble due to numerical errors with finite precision arithmetics. In particular, triangles of certain types of flat tetrahedra called *slivers* tend to contribute to these numerical errors and slivers are not uncommon in the Delaunay triangulation of a sample from a surface.

A robust and faster implementation of the function SURFACENEIGHBOR avoids numerical computations by exploiting the combinatorial structure of the Delaunay triangulation. Every triangle in the Delaunay triangulation has two incident tetrahedra if we account for the infinite ones incident to the convex hull triangles. SURFACENEIGHBOR is called with a triple  $(\sigma, t, e)$ . It circles over the tetrahedra and triangles incident to the edge  $e$  starting from  $t$  and going toward the other triangle of  $\sigma$  incident to  $e$ . This circular walk stops when another cocone triangle  $t'$  is reached. If  $t'$  is reached via the tetrahedron  $\sigma'$ , we output the pair  $(\sigma', t')$ . Assuming inductively that  $\sigma$  intersects  $O_{\text{out}}$ , the tetrahedron  $\sigma'$  also intersects  $O_{\text{out}}$ . For example, in Figure 4.5, SURFACENEIGHBOR is passed on the triple  $(\sigma_1, t, e)$  and then it circles through the tetrahedra  $\sigma_1, \sigma_2, \sigma_3$ , and their triangles till it reaches  $t'$ . At this point it returns  $(\sigma_3, t')$  where both  $\sigma_1$  and  $\sigma_3$  lie outside, that is, in  $O_{\text{out}}$ . SURFTRIANGLES with this implementation of SURFACENEIGHBOR is robust since no numerical decisions are involved (see Figure 4.5). Combinatorial computations instead of numerical ones make SURFTRIANGLES fast provided the Delaunay triangulation is given in a form which allows to answer queries for neighboring tetrahedra quickly.

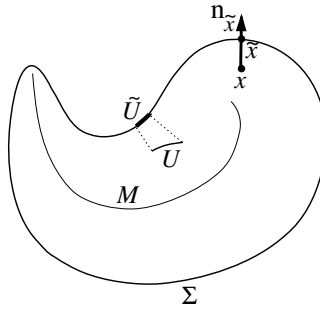


Figure 4.6. Illustration for the map  $\nu$ .

## 4.2 Geometric Guarantees

In this section we establish more properties of the cocone triangles which are eventually used to prove the geometric and topological guarantees of the output of COCONE. We introduce a map  $\nu$  that takes each point  $x \in \mathbb{R}^3$  to its closest point in  $\Sigma$ . Notice that  $\nu$  is well defined everywhere in  $\mathbb{R}^3$  except at the medial axis  $M$  of  $\Sigma$ . Mathematically,  $\nu : \mathbb{R}^3 \setminus M \rightarrow \Sigma$  where  $\nu(x) \in \Sigma$  is closest to  $x$ . Observe that the line containing  $x$  and  $\nu(x)$  is normal to  $\Sigma$  at  $x$ . The map  $\nu$  will be used at many places in this chapter and the chapters to follow. Let

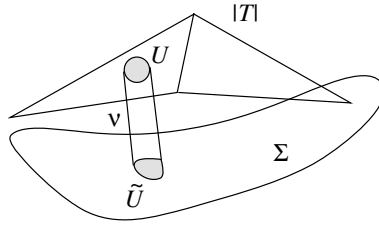
$$\begin{aligned}\tilde{x} &= \nu(x) \text{ for any point } x \in \mathbb{R}^3 \setminus M \text{ and} \\ \tilde{U} &= \{\tilde{x} : x \in U\} \text{ for any set } U \subset \mathbb{R}^3 \setminus M.\end{aligned}$$

See Figure 4.6 for an illustration.

First, we show that all points of the cocone triangles lie close to the surface. This, in turn, allows us to extend the Cocone Triangle Normal Lemma 4.3 to the interior points of the cocone triangles. The restriction of  $\nu$  to the underlying space  $|T|$  of the set of cocone triangles  $T$  is a well-defined function; refer to Figure 4.7. For if some point  $x$  had more than one closest point on the surface when  $\varepsilon \leq 0.05$ ,  $x$  would be a point of the medial axis giving  $\|p - x\| \geq f(p)$  for any vertex  $p$  of a triangle in  $T$ ; but by the Small Triangle Lemma 4.2 every point  $q \in |T|$  is within  $\frac{1.18\varepsilon}{1-\varepsilon} f(p)$  distance of a triangle vertex  $p \in \Sigma$  for  $\varepsilon \leq 0.05$ .

In the next two lemmas and also later we use the notation  $\tilde{O}(\varepsilon)$  defined in Section 1.2.3.

**Lemma 4.4.** *Let  $q$  be any point in a cocone triangle  $t \in T$ . The distance between  $q$  and the point  $\tilde{q}$  is  $\tilde{O}(\varepsilon)f(\tilde{q})$  and is at most  $0.08f(\tilde{q})$  for  $\varepsilon \leq 0.05$ .*

Figure 4.7. The map  $\nu$  restricted to  $|T|$ .

*Proof.* By the Small Triangle Lemma 4.2 the circumradius of  $t$  is at most  $\mu f(p)$  where  $\mu = \frac{1.18\varepsilon}{1-\varepsilon} \leq .07$  and  $p$  is any of its vertices. Let  $p$  be a vertex of  $t$  subtending a maximal angle of  $t$ . Since there is a sample point, namely a vertex of  $t$ , within  $\mu f(p)$  distance from  $q$ , we have  $\|q - \tilde{q}\| \leq \mu f(p)$ . We are interested in expressing this bound in terms of  $f(\tilde{q})$ , so we need an upper bound on  $\|p - \tilde{q}\|$ .

The triangle vertex  $p$  has to lie outside the medial balls at  $\tilde{q}$ , while, since  $\tilde{q}$  is the nearest surface point to  $q$ ,  $q$  must lie on the segment between  $\tilde{q}$  and the center of one of these medial balls. For any fixed  $\|p - q\|$ , these facts imply that  $\|p - \tilde{q}\|$  is maximized when the angle  $\angle pq\tilde{q}$  is a right angle. Thus,  $\|p - \tilde{q}\| \leq \sqrt{5}\mu f(p) \leq 0.14f(p)$  for  $\varepsilon \leq 0.05$ . This implies that  $f(p) = \tilde{O}(\varepsilon)f(\tilde{q})$  and in particular  $f(p) \leq 1.17f(\tilde{q})$  by Lipschitz property of  $f$ . We have  $\|q - \tilde{q}\| \leq \mu f(p) = \tilde{O}(\varepsilon)f(\tilde{q})$  and  $\|q - \tilde{q}\| \leq 0.08f(\tilde{q})$  in particular. ■

With a little more work, we can also show that the triangle normal agrees with the surface normal at  $\tilde{q}$ .

**Lemma 4.5.** *Let  $q$  be a point on triangle  $t \in T$ . The angle  $\angle(\mathbf{n}_{\tilde{q}}, \mathbf{n}_p)$  is at most  $14^\circ$  where  $p$  is a vertex of  $t$  with a maximal angle. Also, the angle  $\angle_a(\mathbf{n}_{\tilde{q}}, \mathbf{n}_t)$  is  $\tilde{O}(\varepsilon)$  and is at most  $38^\circ$  for  $\varepsilon \leq 0.05$ .*

*Proof.* We have already seen in the proof of Lemma 4.4 that  $\|p - \tilde{q}\| = \tilde{O}(\varepsilon)f(p)$ . In particular,  $\|p - \tilde{q}\| \leq 0.14f(p)$  when  $\varepsilon \leq 0.05$ . Applying the Normal Variation Lemma 3.3, and taking  $\rho = \tilde{O}(\varepsilon)$  ( $\rho = 0.14$  in particular), shows that the angle between  $\mathbf{n}_{\tilde{q}}$  and  $\mathbf{n}_p$  is  $\tilde{O}(\varepsilon)$  and is less than  $14^\circ$ . The angle between  $\mathbf{n}_t$  and  $\mathbf{n}_p$  is  $\tilde{O}(\varepsilon)$  and is less than  $24^\circ$  for  $\varepsilon \leq 0.05$  by the Cocone Triangle Normal Lemma 4.3. Thus, the triangle normal and  $\mathbf{n}_{\tilde{q}}$  make  $\tilde{O}(\varepsilon)$  angle which is at most  $38^\circ$  for  $\varepsilon \leq 0.05$ . ■

Lemma 4.2, Lemma 4.4, and Lemma 4.5 imply that the output surface  $|E|$  of COCONE is close to  $\Sigma$  both point-wise and normal-wise. The following theorem states this precisely.

**Theorem 4.2.** *The surface  $|E|$  output by COCONE satisfies the following geometric properties for  $\varepsilon \leq 0.05$ .*

- (i) *Each point  $p \in |E|$  is within  $\tilde{O}(\varepsilon)f(x)$  distance of a point  $x \in \Sigma$ . Conversely, each point  $x \in \Sigma$  is within  $\tilde{O}(\varepsilon)f(x)$  distance of a point in  $|E|$ .*
- (ii) *Each point  $p$  in a triangle  $t \in E$  satisfies  $\angle_a(\mathbf{n}_{\bar{p}}, \mathbf{n}_t) = \tilde{O}(\varepsilon)$ .*

#### 4.2.1 Additional Properties

We argued in Section 4.1.4 that the underlying space of the simplicial complex output by COCONE is a 2-manifold. Let  $E$  be this simplicial complex output by COCONE. A pair of triangles  $t_1, t_2 \in E$  are *adjacent* if they share at least one common vertex  $p$ . Since the normals to all triangles sharing  $p$  differ from the surface normal at  $p$  by at most  $24^\circ$  (apply the Cocone Triangle Normal Lemma 4.3), and that normal in turn differs from the pole vector at  $p$  by less than  $7^\circ$  (apply the Pole Lemma 4.1), we can orient the triangles sharing  $p$ , arbitrarily but consistently. We call the normal facing the positive pole the *inside* normal and the normal facing away from it the *outside* normal. Let  $\theta$  be the angle between the two inside normals of  $t_1, t_2$ . We define the angle at which the two triangles meet at  $p$  to be  $\pi - \theta$ .

**PROPERTY I:** Every two adjacent triangles in  $E$  meet at their common vertex at an angle greater than  $\pi/2$ .

Requiring this property excludes manifolds which contain sharp folds and, for instance, flat tunnels. Since the cocone triangles are all nearly perpendicular to the surface normals at their vertices (Cocone Triangle Normal Lemma 4.3) and the manifold extraction step eliminates triangles adjacent to sharp edges,  $E$  has this property.

**PROPERTY II:** Every point in  $P$  is a vertex of  $E$ .

The Restricted Delaunay Theorem 4.1 ensures that the set  $T$  of cocone triangles contains all restricted Delaunay triangles even after the pruning. Therefore at this point  $T$  contains a triangle adjacent to every sample point in  $P$ . Lemma 4.6 below says that each sample point is exposed to the outside for the component of  $T$  to which it belongs. This ensures that at least one triangle is selected for each sample point by the manifold extraction step. This implies that  $E$  has the second property as well.

**Lemma 4.6 (Exposed).** *Let  $p$  be a sample point and let  $m$  be the center of a medial ball  $B$  tangent to  $\Sigma$  at  $p$ . No cocone triangle intersects the interior of the segment  $pm$  for  $\varepsilon \leq 0.05$ .*

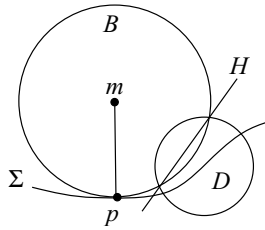


Figure 4.8. Illustration for the exposed lemma.

*Proof.* To intersect the segment  $pm$ , a cocone triangle  $t$  would have to intersect  $B$  and so would the smallest empty ball circumscribing  $t$ . Call it  $D$ . Let  $H$  be the plane of the circle where the boundaries of  $B$  and  $D$  intersect (see Figure 4.8). We argue that  $H$  separates the interior of  $pm$  and  $t$ .

On one side of  $H$ ,  $B$  is contained in  $D$  and on the other,  $D$  is contained in  $B$ . Since the vertices of  $t$  lie on  $\Sigma$  and hence not in the interior of  $B$ ,  $t$  has to lie in the open halfspace, call it  $H^+$ , in which  $D$  is outside  $B$ . Since  $D$  is empty,  $p$  cannot lie in the interior of  $D$ ; but since  $p$  lies on the boundary of  $B$ , it therefore cannot lie in  $H^+$ . We claim that  $m \notin H^+$  either.

Since  $m \in B$ , if it lay in  $H^+$ ,  $m$  would be contained in  $D$ . Since  $m$  is a point of the medial axis, the radius of  $D$  would be at least  $\frac{f(p')}{2}$  for any vertex  $p'$  of  $t$ . For  $\varepsilon \leq 0.05$ , this contradicts the Small Triangle Lemma 4.2. Therefore  $p, m$ , and hence the segment  $pm$  cannot lie in  $H^+$  and  $H$  separates  $t$  and  $pm$ . ■

### 4.3 Topological Guarantee

Recall that a function  $h : \mathbb{X} \rightarrow \mathbb{Y}$  defines a homeomorphism between two compact Euclidean subspaces  $\mathbb{X}$  and  $\mathbb{Y}$  if  $h$  is continuous, one-to-one, and onto. In this section, we will show a homeomorphism between  $\Sigma$  and any piecewise-linear 2-manifold made up of cocone triangles from  $T$ . The piecewise-linear manifold  $E$  selected by the manifold extraction step is such a space thus completing the proof of homeomorphism.

#### 4.3.1 The Map $\nu$

We define the homeomorphism explicitly, using the function  $\nu : \mathbb{R}^3 \setminus M \rightarrow \Sigma$ , as defined earlier. We will consider the restriction  $\nu'$  of  $\nu$  to the underlying space  $|E|$  of  $E$ , that is,  $\nu' : |E| \rightarrow \Sigma$ . Our approach will be first to show that  $\nu'$  is well-behaved on the sample points themselves and then show that this property extends in the interior of each triangle in  $E$ .

**Lemma 4.7.** *For  $\varepsilon \leq 0.05$ ,  $\nu' : |E| \rightarrow \Sigma$  is a well-defined continuous function.*

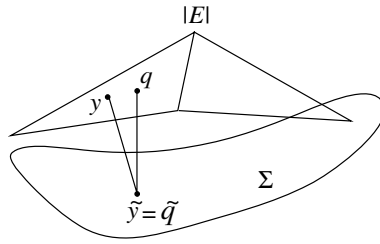


Figure 4.9.  $v'$  maps  $y$  and  $q$  to the same point which is impossible.

*Proof.* By the Small Triangle Lemma 4.2, every point  $q \in |E|$  is within  $\frac{1.18\varepsilon}{1-\varepsilon} f(p)$  of a triangle vertex  $p \in \Sigma$  when  $\varepsilon \leq 0.05$ . Therefore,  $|E| \subset \mathbb{R}^3 \setminus M$  for  $\varepsilon \leq 0.05$ . It follows that  $v'$  is well defined. It is continuous since it is a restriction of a continuous function. ■

Let  $q$  be any point such that  $\tilde{q}$  is a sample point  $p$ . By the Exposed Lemma 4.6,  $q$  lies on the segment  $pm$  where  $m$  is the center of a medial ball touching  $\Sigma$  at  $p$ . We have the following.

**Corollary 4.1.** *For  $\varepsilon \leq 0.05$ , the function  $v'$  is one-to-one from  $|E|$  to every sample point  $p$ .*

In what follows, we will show that  $v'$  is indeed one-to-one on all of  $|E|$ . The proof proceeds in three short steps. We show that  $v'$  induces a homeomorphism on each triangle, then on each pair of adjacent triangles and finally on  $|E|$  as a whole.

**Lemma 4.8.** *Let  $U$  be a region contained within one triangle  $t \in E$  or in adjacent triangles of  $E$ . For  $\varepsilon \leq 0.05$ , the function  $v'$  defines a homeomorphism between  $U$  and  $\tilde{U} \subset \Sigma$ .*

*Proof.* We know that  $v'$  is well defined and continuous on  $U$ , so it only remains to show that it is one-to-one. First, we prove that if  $U$  is in one triangle  $t$ ,  $v'$  is one-to-one. For a point  $q \in t$ , the vector  $\mathbf{n}_q$  from  $\tilde{q}$  to  $q$  is perpendicular to the surface at  $\tilde{q}$ ; since  $\Sigma$  is smooth, the direction of  $\mathbf{n}_q$  is unique and well defined. If there were some  $y \in t$  with  $\tilde{y} = \tilde{q}$ , then  $q$ ,  $\tilde{q}$ , and  $y$  would all be collinear and  $t$  itself would have to contain the line segment between  $q$  and  $y$  (see Figure 4.9). This implies that the normal  $\mathbf{n}_q$  is parallel to the plane of  $t$ . In other words,  $\mathbf{n}_q$  is orthogonal to the normal of  $t$ , contradicting the Cocone Triangle Normal Lemma 4.3 which says that the normal of  $t$  is nearly parallel to  $\mathbf{n}_q$ .



Now, we consider the case in which  $U$  is contained in more than one triangle. Let  $q$  and  $y$  be two points in  $U$  such that  $\tilde{q} = \tilde{y} = x$  and let  $v$  be a common vertex of the triangles that contain  $U$ . Since  $v'$  is one-to-one in one triangle,  $q$  and  $y$  must lie in the two distinct triangles  $t_q$  and  $t_y$ . The line  $l$  through  $x$  with direction  $\mathbf{n}_x$  pierces the patch  $U$  at least twice; if  $y$  and  $q$  are not adjacent intersections along  $l$ , redefine  $q$  so that this is true ( $\tilde{q} = x$  for any intersection  $q$  of  $l$  with  $U$ ). Now consider the orientation of the patch  $U$  according to the direction to the positive pole at  $v$ . Either  $l$  passes from inside to outside and back to inside when crossing  $y$  and  $q$ , or from outside to inside and back to outside.

The acute angles between the triangle normals of  $t_q$ ,  $t_y$ , and  $\mathbf{n}_x$  are less than  $38^\circ$  (Lemma 4.5), that is, the triangles are stabbed nearly perpendicularly by  $\mathbf{n}_x$ . But since the orientation of  $U$  is opposite at the two intersections, the angle between the two *oriented* triangle normals is greater than  $104^\circ$ , meaning that  $t_q$  and  $t_y$  must meet at  $v$  at an acute angle. This would contradict PROPERTY I, which is that  $t_q$  and  $t_y$  meet at  $v$  at an obtuse angle. Hence, there are no two points  $y, q$  in  $U$  with  $\tilde{q} = \tilde{y}$ . ■

### 4.3.2 Homeomorphism Proof

We finish the proof for homeomorphism guarantee using a theorem from topology.

**Theorem 4.3 (Homeomorphism).** *The map  $v'$  defines a homeomorphism from the surface  $|E|$  computed by COCONE to the surface  $\Sigma$  for  $\varepsilon \leq 0.05$ .*

*Proof.* Let  $\Sigma' \subset \Sigma$  be  $v'(|E|)$ . We first show that  $(|E|, v')$  is a *covering space* of  $\Sigma'$ . Informally,  $(|E|, v')$  is a covering space for  $\Sigma'$  if  $v'$  maps  $|E|$  onto  $\Sigma'$ , with no folds or other singularities. Showing that  $(|E|, v')$  is a covering space is weaker than showing that  $v'$  defines a homeomorphism, since, for instance, it does not preclude several connected components of  $|E|$  mapping onto the same component of  $\Sigma'$ , or more interesting behavior, such as a torus wrapping twice around another torus to form a *double covering*.

For a set  $X \subseteq \Sigma'$ , let  $\tau(X)$  denote the set in  $|E|$  so that  $v'(\tau(X)) = X$ . Formally, the  $(|E|, v')$  is a covering space of  $\Sigma'$  if, for every  $x \in \Sigma'$ , there is a path-connected *elementary neighborhood*  $V_x$  around  $x$  such that each path-connected component of  $\tau(V_x)$  is mapped homeomorphically onto  $V_x$  by  $v'$ .

To construct such an elementary neighborhood, note that the set of points  $\tau(x)$  corresponding to a point  $x \in \Sigma'$  is nonzero and finite, since  $v'$  is one-to-one on each triangle of  $E$  and there are only a finite number of triangles. For each point  $q \in \tau(x)$ , we choose an open neighborhood  $U_q$  of  $q$ , homeomorphic to a

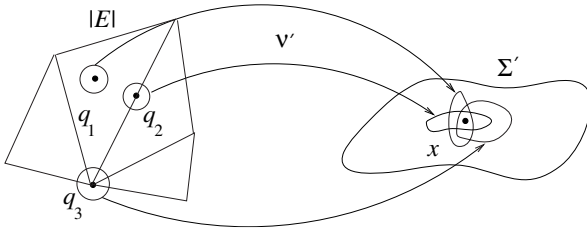


Figure 4.10. Proof of the Homeomorphism Theorem 4.3;  $\tau(x) = \{q_1, q_2, q_3\}$ .

disk and small enough so that  $U_q$  is contained only in triangles that contain  $q$ . (see Figure 4.10).

We claim that  $v'$  maps each  $U_q$  homeomorphically onto  $\tilde{U}_q$ . This is because it is continuous, it is onto  $\tilde{U}_q$  by definition, and, since any two points  $x$  and  $y$  in  $U_q$  are in adjacent triangles, it is one-to-one by Lemma 4.8.

Let  $U'(x) = \bigcap_{q \in \tau(x)} v'(U_q)$ , the intersection of the maps of each of the  $U_q$ .  $U'(x)$  is the intersection of a finite number of open neighborhoods, each containing  $x$ , so we can find an open disk  $V_x$  around  $x$ .  $V_x$  is path connected and each component of  $\tau(V_x)$  is a subset of some  $U_q$  and hence is mapped homeomorphically onto  $V_x$  by  $v'$ . Thus,  $(|E|, v')$  is a covering space for  $\Sigma'$ .

We now show that  $v'$  defines a homeomorphism between  $|E|$  and  $\Sigma'$ . Since  $v': |E| \rightarrow \Sigma'$  is onto by definition, we need only that  $v'$  is one-to-one. Consider one connected component  $G$  of  $\Sigma'$ . A theorem of algebraic topology says that when  $(|E|, v')$  is a covering space of  $\Sigma'$ , the sets  $\tau(x)$  for all  $x \in G$  have the same cardinality. We now use Corollary 4.1, that  $v'$  is one-to-one at every sample point. Since each connected component of  $\Sigma$  contains some sample points, it must be the case that  $v'$  is everywhere one-to-one and  $|E|$  and  $\Sigma'$  are homeomorphic.

Finally, we show that  $\Sigma' = \Sigma$ . Since  $|E|$  is a 2-manifold without boundary and is compact,  $\Sigma'$  must be as well. So,  $\Sigma'$  cannot include part of a connected component of  $\Sigma$ , and hence  $\Sigma'$  must consist of a subset of the connected components of  $\Sigma$ . Since every connected component of  $\Sigma$  contains a sample  $p$  (actually many sample points) and  $v'(p) = p$ , all components of  $\Sigma$  belong to  $\Sigma'$ . Therefore,  $\Sigma' = \Sigma$  and  $|E|$  and  $\Sigma$  are homeomorphic. ■

It can also be shown that  $|E|$  and  $\Sigma$  are isotopic (Exercise 7). We will show a technique to prove isotopy in Section 6.1.3.

#### 4.4 Notes and Exercises

The problem of reconstructing surfaces from samples dates back to the early 1980s. First, the problem appeared in the form of contour surface reconstruction

in medical imaging. A set of cross sections obtained via CAT scan or MRI need to be joined with a surface in this application. The points on the boundary of the cross sections are already joined by a polygonal curve. The problem is to connect these curves in consecutive cross sections. A dynamic programming-based solution for two such consecutive curves was first proposed by Fuchs, Kedem, and Uselton [51]. A result by Gitlin, O'Rourke, and Subramanian [57] shows that, in general, two polygonal curves cannot be joined by nonself intersecting surface with only those vertices; even deciding its possibility is NP-hard. Several solutions with the addition of Steiner points have been proposed to overcome the problem, see Meyers, Skinner, and Sloan [68]. A Delaunay-based solution for the problem was proposed by Boissonnat [15] which is the first Delaunay-based algorithm proposed for a surface reconstruction problem. Later the Delaunay-based method was refined by Boissonnat and Geiger [17] and Cheng and Dey [22].

The most general version of surface reconstruction where no input information other than the point coordinates is used became popular to handle the data from range and laser scanners. In the context of computer graphics and vision, this problem has been investigated intensely in the past decade with emphasis on practical performance. The early work by Hoppe et al. [61], Curless and Levoy [26] and the recent works by Alexa et al. [1], Carr et al. [18], and Ohtake et al. [73] are a few such examples. The  $\alpha$ -shape by Edelsbrunner and Mücke [47] is the first popular Delaunay-based surface reconstruction method. It is the generalization of the  $\alpha$ -shape concept described in Section 2.4 of Chapter 2. Depending on an input parameter  $\alpha$ , Delaunay simplices are filtered based on their circumscribing Delaunay ball sizes. The main drawback of this method is that it is not suitable for nonuniform samples. Also, with the uniform samples, the user is burdened with the selection of an appropriate  $\alpha$ .

The first algorithm for surface reconstruction with proved guarantees was devised by Amenta and Bern [4]. They generalized the CRUST algorithm for curve reconstruction to the surface reconstruction problem. The idea of poles and approximating the normals with the pole vector was a significant breakthrough. The crust triangles (Exercise 2) enjoy some nice properties that help the reconstruction. The COCONE algorithm as described here is a successor of CRUST. Devised by Amenta, Choi, Dey, and Leekha [6], this algorithm simplified the CRUST algorithm and its proof of correctness. COCONE eliminated one of the two Voronoi diagram computations of CRUST and also a normal filtering step. The homeomorphism between the reconstructed surface and the original sampled surface was first established by Amenta et al. [6]. Boissonnat and Cazals [16] devised another algorithm for surface reconstruction using the natural neighbor coordinates (see Section 9.7) and proved its correctness using the framework of CRUST. Since the Deluanay triangulations of  $n$  points in three

dimensions take  $O(n^2)$  time and space in the worst case, the complexity of all these algorithms is  $O(n^2)$ . Funke and Ramos [53] showed how the COCONE algorithm can be adapted to run in  $O(n \log n)$  time. Unfortunately, the modified algorithm is not very practical.

Although the Delaunay triangulation of  $n$  points in three dimensions may produce  $\Omega(n^2)$  simplices in the worst case, such complexities are rarely observed for point samples of surfaces in practice. Erickson [49] started the investigation of determining the complexity of the Delaunay triangulations for points on surfaces. Attali, Boissonnat, and Lieutier [10] proved that indeed the Delaunay triangulation has  $O(n \log n)$  complexity if the point sample is locally uniform for a certain class of smooth surfaces.

### Exercises

1. We know that Voronoi vertices for a dense sample from a curve in the plane lie near the medial axis. The same is not true for surfaces in three dimensions. Show an example where a Voronoi vertex for an arbitrarily dense sample lies arbitrarily close to the surface.
- 2<sup>h</sup>. Let  $P$  be a sample from a  $C^2$ -smooth surface  $\Sigma$  and  $V$  be the set of poles in  $\text{Vor } P$ . Consider the following generalization of the CRUST. A triangle in the  $\text{Del}(P \cup V)$  is a *crust* triangle if all of its vertices are in  $P$ . Show the following when  $P$  is an  $\varepsilon$ -sample for a sufficiently small  $\varepsilon$ .
  - (i) All restricted Delaunay triangles in  $\text{Del}(P \cup V)|_\Sigma$  are crust triangles.
  - (ii) All crust triangles have circumradius  $\tilde{O}(\varepsilon)f(p)$  where  $p$  is a vertex of the triangle.
3. Let  $t$  be a triangle in  $\text{Del } P$  where  $B = B_{v,r}$  and  $B' = B'_{v',r'}$  are two Delaunay balls circumscribing  $t$ . Let  $x$  be any point on the circle where the boundaries of  $B$  and  $B'$  intersect. Show that, if  $\angle vxv' > \frac{\pi}{2}$ , the triangle normal of  $t$  makes an angle of  $\tilde{O}(\varepsilon)$  with the normals to  $\Sigma$  at its vertices when  $P$  is an  $\varepsilon$ -sample of  $\Sigma$  for a sufficiently small  $\varepsilon$ .
4. Recall that  $P$  is a locally  $(\varepsilon, \delta)$ -uniform sample of a smooth surface  $\Sigma$  if  $P$  is an  $\varepsilon$ -sample of  $\Sigma$  and each sample point  $p \in P$  is at least  $\frac{\varepsilon}{\delta}f(p)$  distance away from all other points in  $P$  where  $\delta > 1$  is a constant. Show that each triangle in the surface output by COCONE for such a sample has a bounded aspect ratio (circumradius to edge length ratio). Also, prove that each vertex has no more than a constant number (determined by  $\varepsilon$  and  $\delta$ ) of triangles on the surface.
- 5<sup>h</sup>. Let  $t$  be a cocone triangle. We showed that any point  $x \in t$  is  $\tilde{O}(\varepsilon)f(\tilde{x})$  away from its closest point  $\tilde{x}$  in  $\Sigma$ . Prove that the bound can be improved to  $\tilde{O}(\varepsilon^2)f(\tilde{x})$ .

6. We defined a Delaunay triangle  $t$  as a cocone triangle if dual  $t$  intersects cocones of *all* of its three vertices. Relax the condition by defining  $t$  as a cocone triangle if dual  $t$  intersects the cocone of *any* of its vertices. Carry out the proofs of different properties of cocone triangles with this modified definition.
7. We showed that the surface  $|E|$  computed by COCONE is homeomorphic to  $\Sigma$  when  $\varepsilon$  is sufficiently small. Prove that  $|E|$  is indeed isotopic to  $\Sigma$ .